NACA TN 2015

NATIONAL ADVISORY COMMITTEE FOR AERONAUTICS

TECHNICAL NOTE 2015

WATER LANDING INVESTIGATION OF A MODEL HAVING A HEAVY BEAM LOADING AND A 30° ANGLE OF DEAD RISE

By Sidney A. Batterson and A. Ethelda McArver

Langley Aeronautical Laboratory
Langley Air Force Base, Va.

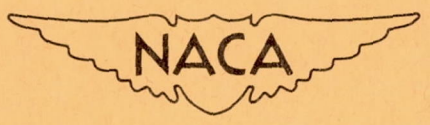

Washington
February 1950

NATIONAL ADVISORY COMMITTEE FOR AERONAUTICS

TECHNICAL NOTE 2015

WATER LANDING INVESTIGATION OF A MODEL HAVING A HEAVY BEAM LOADING AND A 30° ANGLE OF DEAD RISE

By Sidney A. Batterson and A. Ethelda McArver

SUMMARY

A model having a heavy beam loading and an angle of dead rise of 30° was subjected to smooth-water impacts in the Langley impact basin. The tests were made at fixed trims of 6°, 15°, 30°, and 45° for a range of flight-path angles from approximately 2° to 22°. The beam-loading coefficient (18.8) was constant throughout the test.

Time histories of horizontal and vertical displacements, vertical velocity, vertical acceleration, and pitching moment were obtained. The results are presented as plots showing the variation of the experimentally determined quantities converted to nondimensional coefficients with the flight-path angle at water contact. Throughout the tests maximum acceleration occurred subsequent to chine immersion. The impact lift coefficient increased with trim up to 30°; however, no change was apparent between the trims of 30° and 45°. Throughout the range of these tests the draft appeared to be solely a function of flight-path angle.

INTRODUCTION

Interest in the hydrodynamic characteristics of configurations having heavy beam loadings has been stimulated recently by both the development of high-length-beam-ratio flying boats and the considerations being given to the use of hydroflaps as a means for alleviating some of the take-off and landing problems posed by high-speed aircraft. Theoretical considerations indicate that landings associated with heavy beam loadings will exhibit greater depths of immersion in order to dissipate the vertical momentum. Development of the equations necessary to predict the loads resulting from immersion of such configurations has been handicapped by the lack of pertinent experimental data. Even though the theory developed in reference 1 is very general and indicates that the maximum load occurs subsequent to chine immersion for the heavy-beam-loading case, the equations and coefficients developed in references 1 and 2 are limited to landings in which maximum load occurs

before or within a limited range subsequent to chine immersion. In order to convert the equations to a form valid for the heavy-beam-loading case, the theory must be evaluated on the basis of pertinent experimental data to determine the relative importance of the various quantities. The purpose of this paper is to present experimental data that can be used in extending the range of the equations to include substantial amounts of chine immersion.

Tests were conducted in the Langley impact basin with a model having a dead-rise angle of 30°, a beam of 1 foot, and a length of 5 feet. The total weight was 1172 pounds. The tests were made over a very wide trim range in order to simulate landings of aircraft equipped with hydroflaps as well as landings of seaplanes having high length-beam ratios. This paper presents test results and discusses the effects of various parameters.

SYMBOLS

β	angle of dead rise, degrees
γ	flight-path angle relative to undisturbed water surface, degrees
ρ	density of water (1.938 slugs/cu ft)
τ	trim angle, degrees
b	model beam, feet
g	acceleration due to gravity (32.2 fps)
l	wetted keel length, feet ($y/\sin \tau$)
M	pitching moment, pound-feet
n_{i_w}	impact load factor, measured normal to undisturbed water surface, g units
t	time after contact, seconds
V	resultant velocity of model, feet per second
W	dropping weight, pounds
w	specific weight of water (62.4 lb/cu ft)

$\dot{x}$ velocity of model parallel to undisturbed water surface, feet per second

y immersion of model normal to undisturbed water surface, feet

$\dot{y}$ velocity of model normal to undisturbed water surface, feet per second

c_p distance from reference to center of pressure, feet

$\varphi(A)$ aspect-ratio correction factor

Subscripts:

o at water contact

f referred to front fittings

s referred to step

max maximum

Dimensionless variables:

C_l impact lift coefficient $\left(\frac{n_{i_w} W}{\frac{1}{2}\rho V_o^2 b^2}\right)$

C_d draft coefficient $\left(\frac{Y}{b}\right)$

C_t time coefficient $\left(\frac{V_o t}{b}\right)$

C_M pitching-moment coefficient $\left(\frac{M}{\frac{1}{2}\rho V_o^2 b^3}\right)$

C_{cp} center-of-pressure coefficient $\left(\frac{c_p}{b}\right)$

C_Δ beam-loading coefficient $\left(\frac{W}{wb^3}\right)$

APPARATUS

The investigation was conducted in the Langley impact basin with the test equipment and instrumentation described in reference 3. The test model was 1 foot wide and had a dead-rise angle of 30° and a prismatic section for a length of 5 feet. The model was constructed of mild steel, the parts of which were welded together, and was designed so that the strength of the model was such that any structural deformations under load were negligible. The lines and pertinent dimensions of the model are shown in figure 1 and a photograph of the model is presented as figure 2.

The model was rigidly attached to a load-measuring dynamometer which in turn was attached to the carriage boom. Variations in trim were obtained by utilizing various lengths of trim links between the rear attachment point of the dynamometer and boom (fig. 2).

The instrumentation used to measure both the vertical displacement and velocity and the horizontal displacement and velocity was described in reference 3. Accelerations in the vertical direction were measured by a standard NACA air-damped accelerometer having a range of -1g to 6g and a natural frequency of 16.5 cycles per second with approximately 0.65 of the critical damping. The initial water contact and water exit of the model were determined by means of an electrical circuit completed by the water. Complete time histories of the parameters were obtained on a recording oscillograph. A sample record is shown in figure 3.

PRECISION

The apparatus used in the present investigation gives measurements that are believed correct within the following limits:

Horizontal velocity, feet per second	±0.5
Vertical velocity at contact, feet per second	±0.2
Vertical displacement, feet	±0.02
Acceleration, percent	±5
Time, seconds	±0.005
Weight, pounds	±2.0
Pitching moment about front fittings, percent	±5

TEST PROCEDURE

The model was tested at 0° yaw and at trims of 6°, 15°, 30°, and 45° in smooth water. The horizontal velocity for these tests ranged from approximately 25 to 90 feet per second, and the vertical velocity ranged from approximately 3 to 10 feet per second. The depth of immersion of the model was measured from the instant of initial water contact and in a direction perpendicular to the undisturbed water surface. During the impact process, a lift force equal to the total weight of the model and drop linkage was exerted on the float by means of the lift engine described in reference 3.

The pitching moment was measured by the dynamometer, the construction of which was such that pitching moment about the front fittings of the model (fig. 1) was measured directly. The vertical load was measured by both the dynamometer and an accelerometer located on the boom. Comparing the values from both instruments showed that very good agreement was obtained; however, since the data obtained with the accelerometer appeared to have less scatter than those obtained with the dynamometer, the accelerometer results were used in working up the test data presented in this paper.

Particular care was exercised during the test to insure that only the prismatic section of the model was immersed. The limiting condition was reached by making the initial runs for each trim at the lowest flight-path angle obtainable. The flight-path angle was then progressively increased until the immersion of the model was such that a further increase in flight-path angle would have caused the bow to enter the water.

The model together with the drop linkage weighed 1172 pounds; however, they were in turn attached to a carriage weighing 5600 pounds. This condition affected the motion of the model in that the drag forces acting on the model did not develop the horizontal acceleration that would have resulted in the absence of the carriage mass. The hydrodynamic equations appearing in references 1 and 2 are in a form which permit separation of the horizontal and vertical mass. The values of the horizontal and vertical mass were substituted into the equations and the solutions compared with solutions for which this mass inequality did not exist. Although the solutions are strictly valid only for the infinite-beam

float, the results are believed to approximate the error which can be expected in these tests, and the range in which it is most serious. The results of the calculations showed that the carriage-mass effects cause the largest discrepancies at the high trims and high flight-path angles; however, the discrepancies in maximum load did not exceed 5 percent throughout the trim range and flight-path-angle range covered during these tests.

RESULTS AND DISCUSSION

The values of the independent as well as the dependent experimental parameters are presented in table I. The test results are also presented as plots showing the variation of the experimentally determined quantities converted to nondimensional coefficients with the initial flight-path angle γ_o. Since the nondimensional coefficients employed do not include values affected by changes in geometry and loading, the results are valid only for a prismatic form having a dead-rise angle of 30° and a beam-loading coefficient of 18.8. Use of the coefficients presented in reference 2 is not feasible since they are based on the equations presented in reference 1, and, as such, contain relationships specified by the equations. The theoretical equations are for the case of a prismatic section with infinite beam and are valid only when the chines are not immersed. For this condition, the shape of the wetted area projected in the plane of the undisturbed water surface will obviously be a triangle for a prismatic body having a constant dead-rise angle (fig. 4(a)). If, however, chine immersion occurs during impacts of a prismatic form having a constant dead-rise angle, the projected area takes the form of a triangle in the forward portion with a rectangle attached to it as shown in figure 4(b). Very good agreement was obtained in references 1 and 2 between the theoretical equations and the experimental results when an aspect-ratio correction factor $\varphi(A) = 1 - \frac{\tan \tau}{2 \tan \beta}$ was used in the solutions for impacts in which the chines were not immersed. Since the trim was assumed to remain constant throughout the immersion, the aspect-ratio factor was also a constant throughout the immersion. It is uncertain whether the aspect-ratio correction factor in this form is valid for the immersions having projected wetted areas including both the triangular and rectangular forms. Furthermore, the increase of the virtual mass in the rectangular portion will differ from that resulting in the triangular portion and thereby further affect the net impact load predicted by the infinite-beam equations.

Figure 5 shows a plot of the impact lift coefficient against flight-path angle at water contact. Inasmuch as the lift engine contributed a

force equal to the dropping weight, 1 g was subtracted from the values obtained from the accelerometer records used in determining $\left(n_{i_w}\right)_{max}$ in order to isolate the hydrodynamic impact force. Figure 5 shows that the impact lift coefficient increases with trim up to 30°; however, no change is apparent between the trims of 30° and 45°.

Figure 6 presents the draft coefficient at the instant of maximum displacement and also at the instant of maximum acceleration plotted against flight-path angle at water contact. A curve can be faired through all the test points corresponding to the instant of maximum acceleration and another curve can be faired through those corresponding to the maximum immersion. Therefore, the effect of trim was not pronounced and the draft appears to be a function of the flight-path angle alone throughout the trim range of these tests. Maximum acceleration occurred subsequent to chine immersion and prior to maximum immersion in all cases. This fact is based on the geometric interpretation of the draft coefficient required at each trim to immerse the chines with respect to the undisturbed water surface. If wave rise is considered, chine immersion would occur even sooner. At flight-path angles smaller than those covered during these tests, maximum load could occur prior to chine immersion. The sample oscillograph record presented in figure 3 clearly illustrates the relation between the time of maximum load and chine immersion.

The ratio of the vertical velocity at the instant of maximum acceleration and the vertical velocity at the instant of model exit to the initial vertical velocity is plotted against flight-path angle at water contact in figure 7. The large amount of scatter apparent in the velocity ratio is attributed to the frequency-response errors inherent in the velocity recorder. The scatter present in figure 7 makes it difficult to determine any clearly defined trends of the velocity ratio.

The effect of the flight-path angle at water contact upon the time to reach maximum acceleration, to reach maximum draft, and for the model to exit is shown in figures 8(a), 8(b), and 8(c), respectively. The variation of the time coefficient with flight-path angle at water contact does not appear to be affected by trim up to the time of maximum acceleration (fig. 8(a)); however, at the time of maximum draft the 6° trim results show higher values than the remaining trim results (fig. 8(b)). At the instant of exit (fig. 8(c)), the 15° trim results are observed to have slightly higher values than the 30° and 45° trim results, which still fall together.

Figure 9 presents the pitching-moment coefficient at $\left(n_{i_w}\right)_{max}$ about the front fittings against the flight-path angle at water contact. Since the drag forces parallel to the keel are very small, the resultant load is considered to be normal to the keel. Therefore, the

direction of the resultant load is substantially parallel to the center line of the front fittings and the pitching-moment arm can be considered as the distance between the resultant load on the float bottom and the center line of the front fittings. The effect of the inertia force can be neglected because calculations including this effect showed it to be negligible since the model mass below the dynamometer was only a small part of the total dropping weight. The distance of the center of pressure from the center line of the front fitting is therefore obtained from the relation $c_{p_f} = \frac{M_f}{\frac{n_{i_w}}{\cos \tau} W}$.

In order to present the data in a more practical form the distance of the center of pressure from the front fitting (fig. 1) was subtracted from 36.375 inches (converted to feet) and resulted in a value of center-of-pressure distance from the step c_{p_s} for each test run. These values of c_{p_s} obtained at the time of maximum acceleration are divided by the model beam to form nondimensional center-of-pressure coefficients at the time of $\left(n_{i_w}\right)_{max}$ which are plotted against flight-path angle at water contact in figure 10. The scatter in the test data appears rather large. This scatter is largely attributed to the fact that two experimentally determined parameters n_{i_w} and M_f, with the attendant experimental errors of each, were used in obtaining the values of center-of-pressure distance.

The relation $l = \frac{y}{\sin \tau}$ represents the wetted length along the keel of the model providing that water rise along the keel during the immersion is neglected. The ratio $\frac{c_{p_s}}{l}$ is therefore representative of the distance between the step and center of pressure as a proportion of the entire wetted length along the keel. This parameter is plotted against the flight-path angle at water contact in figure 11 by use of the faired values of draft coefficients from figure 6 and center-of-pressure coefficients from figure 10. For the infinite-beam float, the center-of-pressure distance forward of the step was shown to be approximately one-third the wetted keel length (reference 4). Figure 11 shows that the center of pressure occurs substantially forward of the one-third point throughout the entire range tested except for the runs made at 45° trim at the very low flight-path angles. The fact that the center-of-pressure distance is substantially greater than one-third the wetted keel length from the step and even exceeds one-half in most of the runs indicates that a greater proportion of the load occurs in the forward wetted portion (fig. 4(b)). The values of the ratio $\frac{c_{p_s}}{l}$ less than

one-third occurring in figure 11 can only be explained by instrument error. These values were obtained at comparatively small immersions, and slight errors in the measured parameters y, n_{i_w}, and M_f result in apparently large errors in the ratio $\frac{c_{p_s}}{l}$.

The pitching moment at the time of maximum acceleration will differ very little from the maximum pitching moment about the step because the maximum draft was only slightly greater than that occurring at maximum acceleration (fig. 6), and since the vertical load decreased between these two values, the pitching moment changes very little. The variation of the pitching-moment coefficient about the step with flight-path angle at water contact is shown in figure 12. The values of C_{M_s} appearing in figure 12 were derived from the faired values of the impact lift coefficient (fig. 5) and center-of-pressure coefficient (fig. 10).

The runs made at high trims and high speeds showed excessive spray characteristics. Dense clouds of spray were thrown up and reached heights equivalent to approximately four times the over-all model length (approx. 20 ft). However, as the trim and speed were reduced, this condition showed marked improvement.

CONCLUSIONS

Tests were made in the Langley impact basin to obtain experimental data from smooth-water landing tests of a model having a heavy beam loading, an angle of dead rise of 30°, and a beam-loading coefficient of 18.8. The results of the tests which were made at constant weight and at trims of 6°, 15°, 30°, and 45° indicated the following conclusions:

1. Maximum acceleration occurred subsequent to chine immersion throughout these tests.

2. The impact lift coefficient increased with trim up to 30°; however, no change was apparent between the trims of 30° and 45°.

3. The draft appeared to be a function of flight-path angle alone throughout the trim range of these tests.

4. The greater proportion of load was developed on the forward wetted portion of the model throughout most of these tests.

Langley Aeronautical Laboratory
National Advisory Committee for Aeronautics
Langley Air Force Base, Va., November 18, 1949

REFERENCES

1. Mayo, Wilbur L.: Analysis and Modification of Theory for Impact of Seaplanes on Water. NACA Rep. 810, 1945.

2. Milwitzky, Benjamin: A Generalized Theoretical and Experimental Investigation of the Motions and Hydrodynamic Loads Experienced by V-Bottom Seaplanes during Step-Landing Impacts. NACA TN 1516, 1948.

3. Batterson, Sidney A.: The NACA Impact Basin and Water Landing Tests of a Float Model at Various Velocities and Weights. NACA Rep. 795, 1944.

4. Milwitzky, Benjamin: A Generalized Theoretical Investigation of the Hydrodynamic Pitching Moments Experienced by V-Bottom Seaplanes during Step-Landing Impacts and Comparisons with Experiment. NACA TN 1630, 1948.

TABLE I

IMPACT-LOADS DATA FROM TESTS OF A MODEL HAVING A HEAVY BEAM LOADING

Test run	At contact				At $(n_{i_w})_{max}$					At y_{max}		At exit	
	V_o (fps)	$\dot{y}_o$ (fps)	$\dot{x}_o$ (fps)	γ_o (deg)	t (sec)	n_{i_w} (g)	y (ft)	$\dot{y}$ (fps)	M_f (lb-ft)	t (sec)	y (ft)	t (sec)	$\dot{y}$ (fps)
$\tau = 6^\circ$													
1	91.0	2.9	90.9	1.82	0.152	0.6	0.32	1.1	1,088	0.207	0.37	0.492	-1.9
2	89.3	3.0	89.3	1.95	.130	.7	.31	1.5	1,257	.214	.36	.470	-1.6
3	94.2	4.0	94.1	2.41	.095	.9	.29	2.2	1,715	.210	.42	.449	-1.9
$\tau = 15^\circ$													
4	89.4	3.4	89.3	2.16	0.125	1.1	0.32	1.3	3,127	0.160	0.35	0.325	-2.6
5	92.2	3.5	92.2	2.18	-----	---	----	---	3,381	.160	.32	.315	-2.3
6	89.4	3.4	89.3	2.20	.127	1.1	.32	.9	3,127	.161	.34	.324	-2.7
7	92.3	4.1	92.2	2.54	.127	1.2	.34	1.2	3,479	.165	.37	.314	-2.5
8	63.4	3.8	63.3	3.40	.146	.9	.42	1.4	1,993	.214	.45	.476	-2.4
9	91.1	5.7	90.9	3.60	.100	1.6	.44	3.0	4,215	.157	.51	.325	-4.1
10	52.8	4.0	52.6	4.29	.155	.6	.45	1.9	1,507	.250	.54	.595	-2.1
11	90.6	9.3	90.1	5.89	.083	2.4	.61	5.4	4,874	.161	.84	.343	-5.8
12	91.4	9.4	90.9	5.92	.082	2.6	.63	5.9	4,858	.156	.82	.338	-5.9
$\tau = 30^\circ$													
13	97.6	3.6	97.6	2.09	0.114	1.5	0.31	0.8	5,246	0.135	0.31	0.262	-3.1
14	96.1	4.2	96.0	2.47	.100	1.8	.36	1.8	6,077	.134	.39	.258	-4.0
15	92.1	5.1	92.0	3.12	.117	1.7	.36	1.3	6,293	.141	.43	.283	-4.4
16	63.0	4.6	62.9	4.19	.135	1.1	.48	2.0	3,710	.205	.51	.410	-3.2
17	92.7	6.9	92.4	4.29	.090	2.5	.48	3.6	7,968	.151	.54	.274	-6.2
18	91.2	7.4	90.9	4.65	.104	2.3	.57	2.5	7,668	.136	.62	.289	-6.1
19	91.2	7.5	90.9	4.67	.113	2 ½	.61	2.3	7,943	.147	.66	.283	-6.5
20	91.2	7.5	90.9	4.67	.120	2.4	.59	2.0	8,065	.146	.66	.283	-6.3
21	91.2	7.5	90.9	4.74	.104	2.4	.60	3.3	8,004	.143	.66	.283	-6.3
22	91.2	7.6	90.9	4.78	.113	2.4	.62	2.3	7,943	.146	.67	.291	-6.5
23	91.2	7.7	90.9	4.87	.107	2.4	.61	2.7	8,187	.143	.66	.287	-6.4
24	48.6	4.6	48.4	5.43	.190	.8	.66	1.8	2,266	.281	.71	.594	-2.9
25	45.7	6.7	45.2	8.40	.166	1.1	.88	3.3	2,446	.273	1.02	.613	-3.8
26	45.1	7.6	44.4	9.68	.175	1.2	.99	3.2	2,457	.270	1.09	.611	-4.7
27	52.4	9.3	51.6	10.22	.145	1.6	1.08	4.7	3,602	.243	1.26	.538	-5.9
28	50.9	9.4	50.0	10.67	.147	1.5	1.06	4.9	3,403	.253	1.28	.564	-5.6
29	26.7	9.3	25.0	20.38	.237	.9	1.62	4.7	------	.440	2.18	1.240	-3.2
$\tau = 45^\circ$													
30	93.1	3.3	93.0	2.02	0.103	1.3	0.27	1.4	6,542	0.147	0.32	0.276	-3.1
31	92.4	4.5	92.3	2.77	.100	1.6	.36	2.3	7,863	-----	----	.280	----
32	89.5	5.9	89.3	3.75	.128	1.9	.51	1.6	8,553	.150	.52	.291	-5.6
33	91.3	8.3	90.9	5.20	.118	2.6	.70	2.4	10,936	.148	.72	.293	-7.5
34	91.3	8.3	90.9	5.20	.124	2.4	.72	2.4	10,814	.150	.75	.295	-7.3
35	92.2	8.4	91.8	5.24	.117	2.9	.72	2.3	------	.149	.75	.288	-8.2
36	43.5	5.3	43.1	6.94	.201	.8	.79	2.1	2,944	.322	.82	.635	-4.1
37	43.7	7.5	43.0	9.82	.215	1.0	1.13	2.9	3,315	.299	1.19	.654	-4.0
38	51.4	9.5	50.5	10.64	.187	1.5	1.27	3.5	4,767	.257	1.37	.559	-6.8
39	51.4	9.6	50.5	10.72	.186	1.5	1.22	3.6	4,706	.256	1.38	.571	-6.3
40	34.9	8.3	33.9	13.75	.214	.9	1.37	4.2	2,434	.376	1.60	.861	-4.3
41	29.3	9.4	27.8	18.60	.260	.9	1.80	4.4	1,809	.429	2.21	1.072	-4.4
42	24.7	7.9	23.4	18.66	.275	.6	1.67	4.3	1,394	.498	2.05	1.365	-2.3
43	28.8	9.6	27.2	19.37	-----	---	----	---	------	.435	2.25	1.108	-4.3

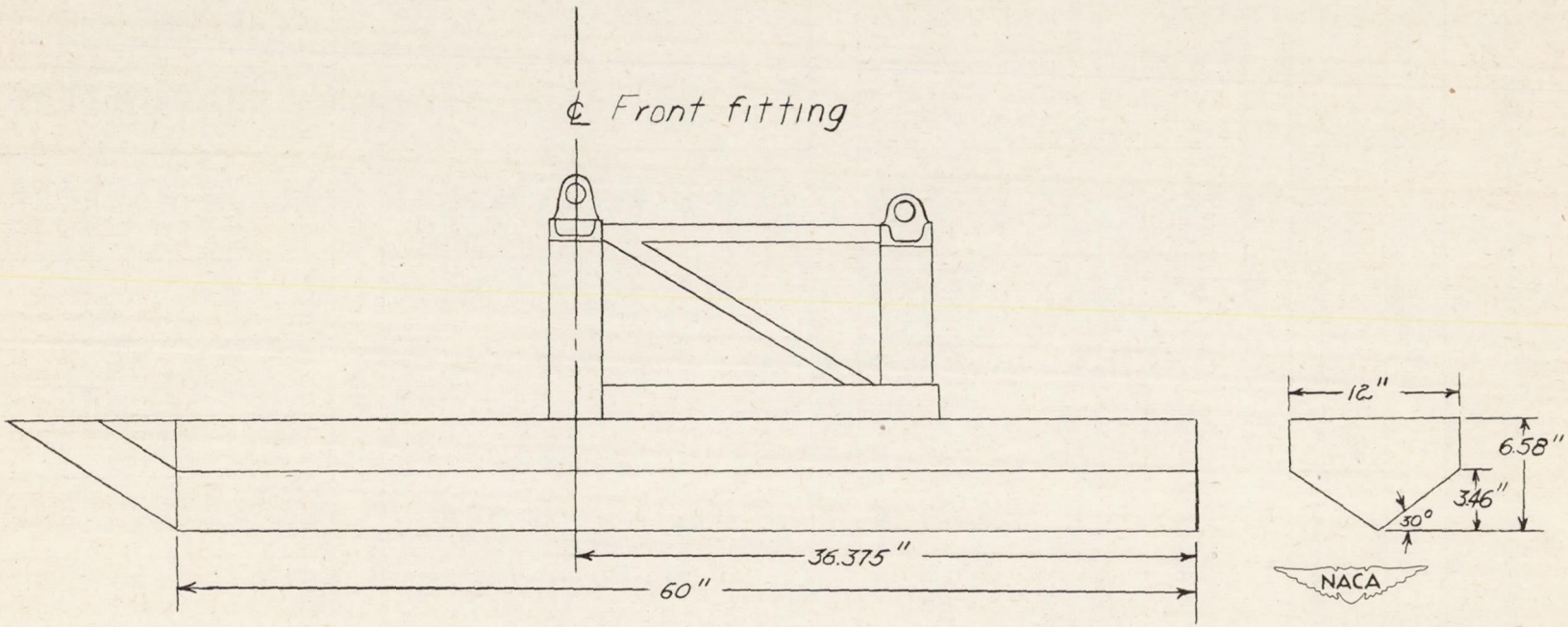

Figure 1.- Lines and pertinent dimensions of model tested in Langley impact basin.

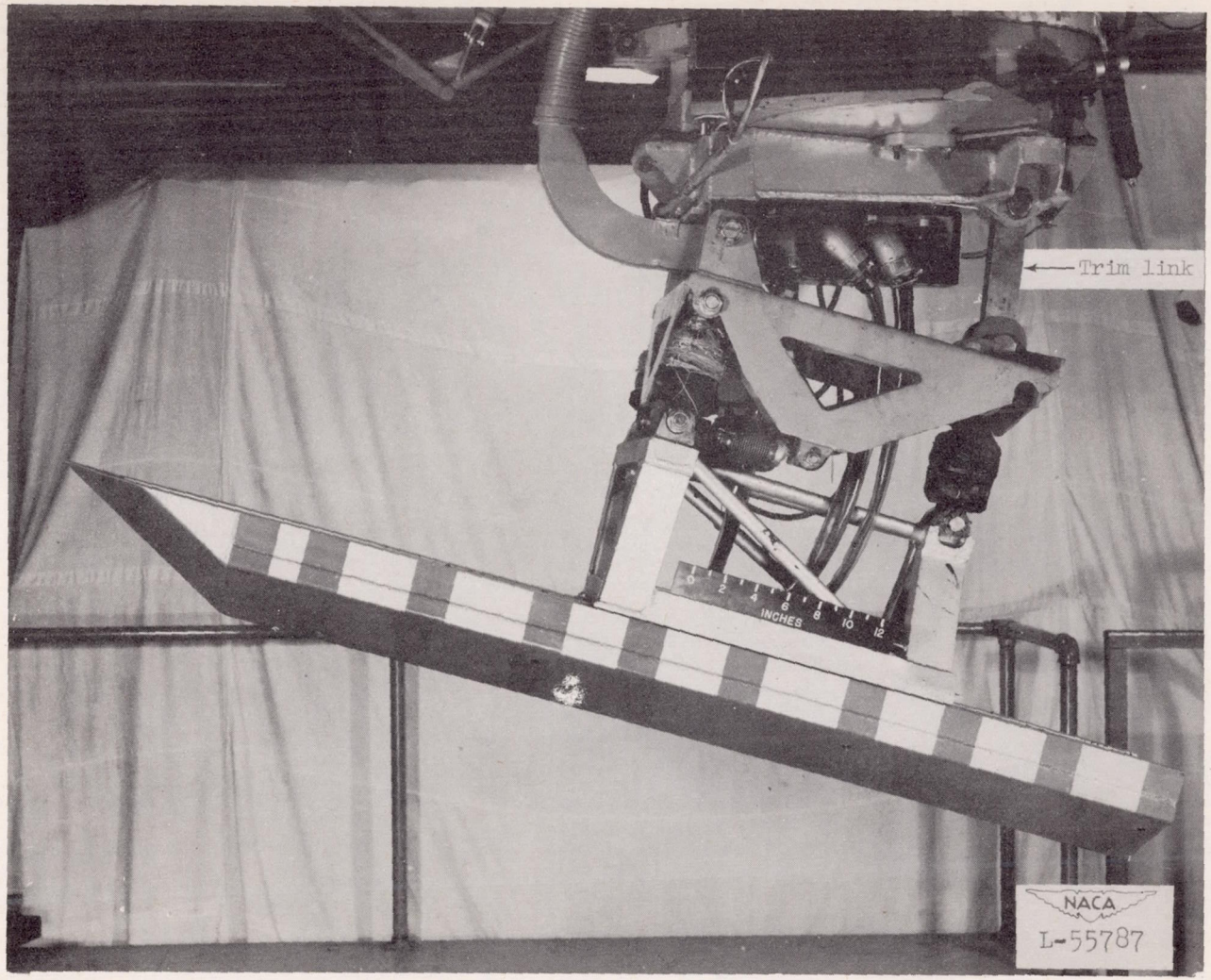

Figure 2.- Model tested in Langley impact basin.

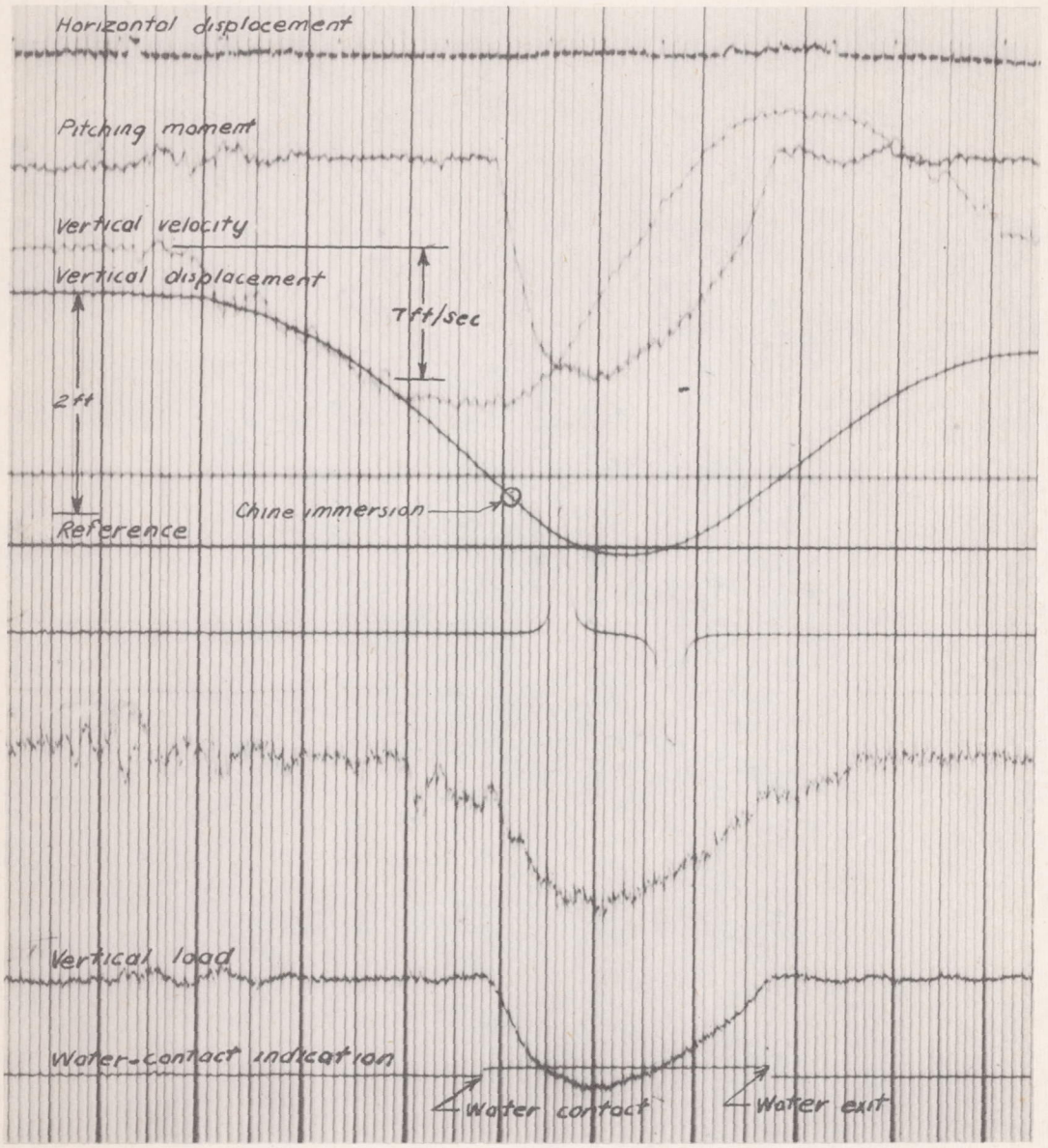

Figure 3.- Typical oscillograph record obtained during test run 33 at the Langley impact basin. $\dot{x}$ = 90.9; $\dot{y}$ = 8.3.

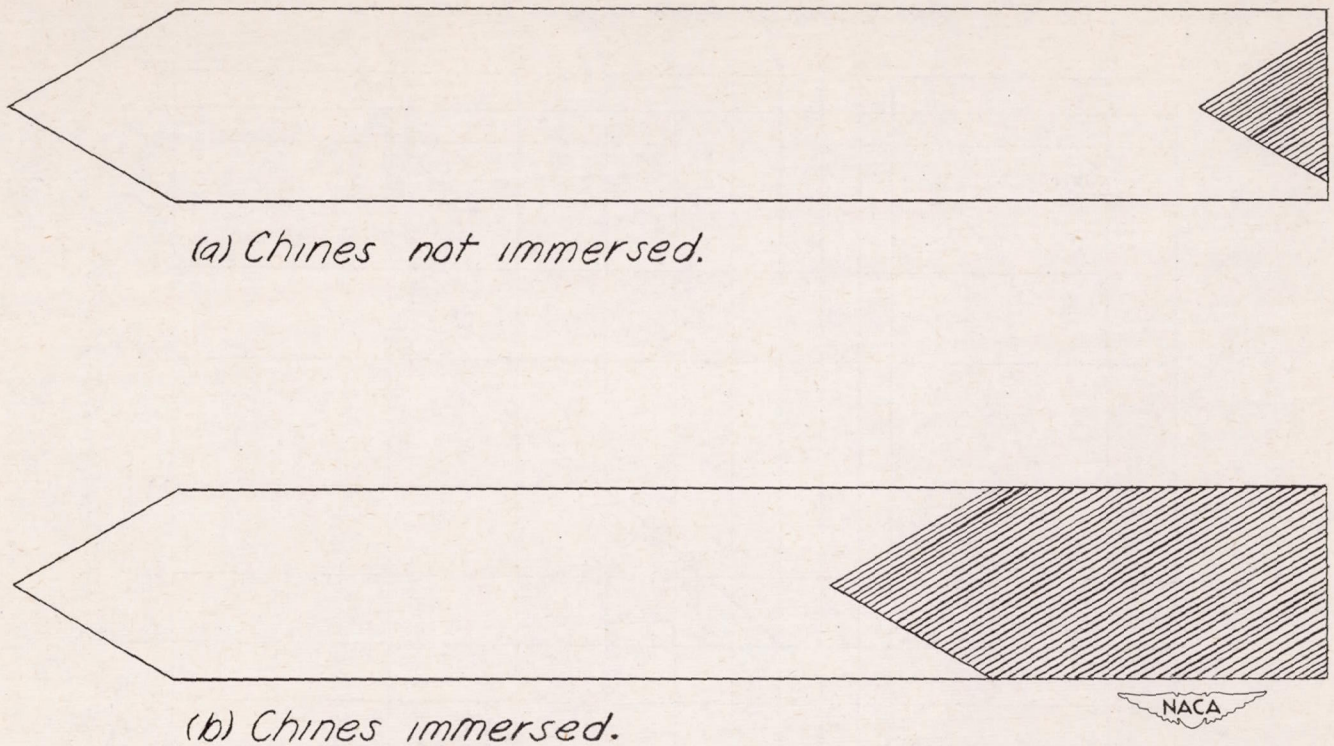

Figure 4.- Wetted areas in plane of undisturbed water surfaces for model at positive trim.

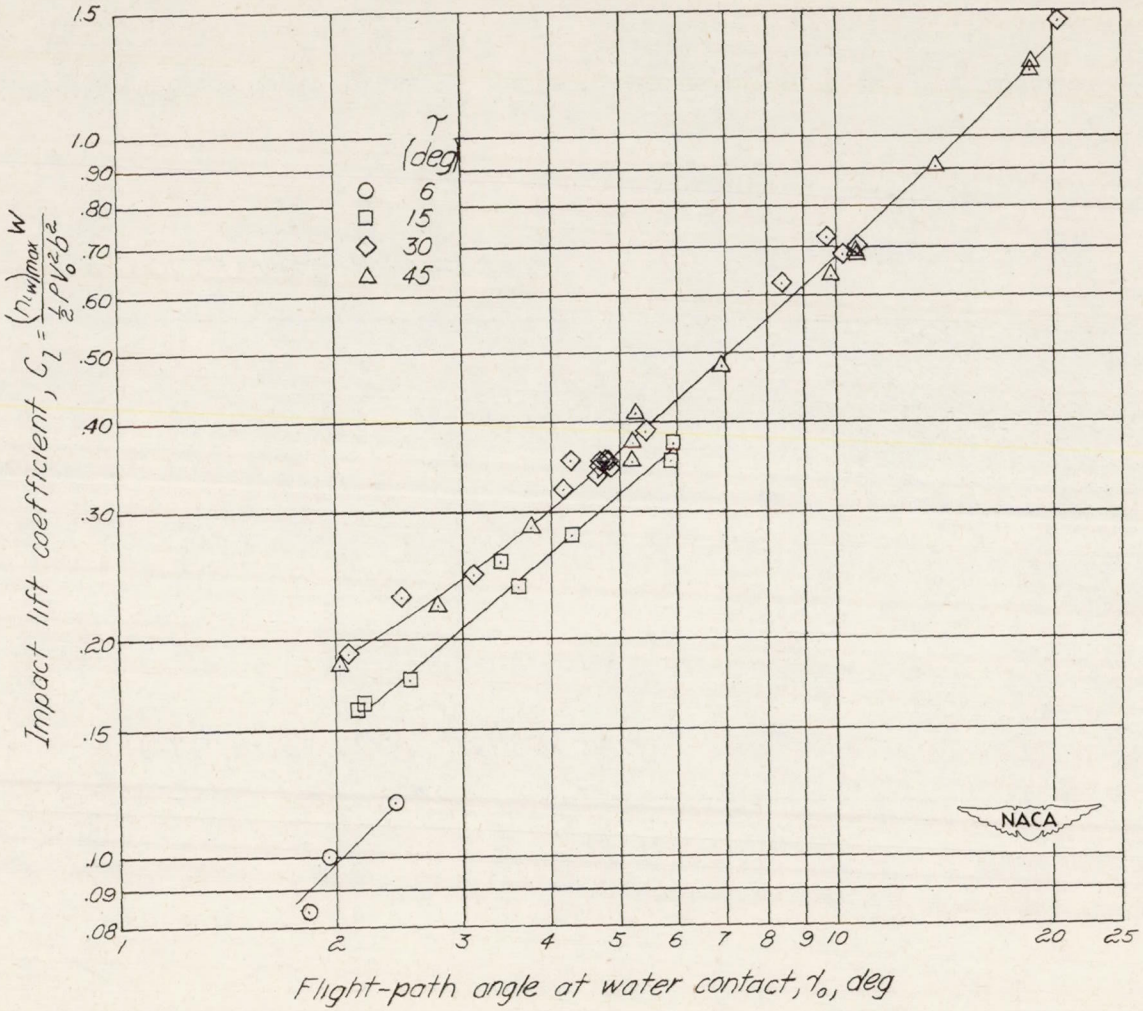

Figure 5.- Variation of impact lift coefficient with flight-path angle at water contact. $\beta = 30^\circ$; $C_\Delta = 18.8$.

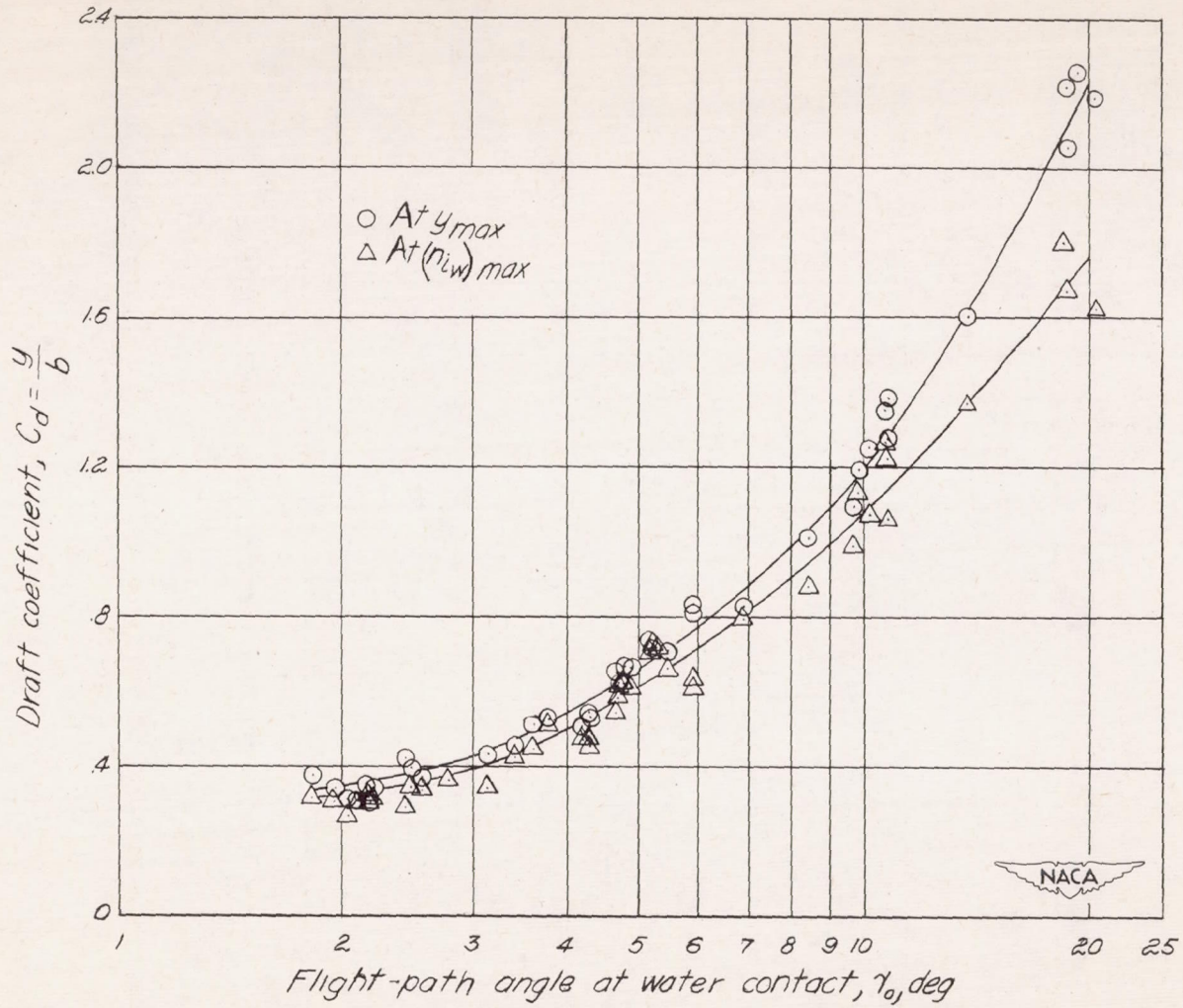

Figure 6.- Variation of draft coefficient with flight-path angle at water contact. $\beta = 30^{\circ}$; $C_{\Delta} = 18.8$.

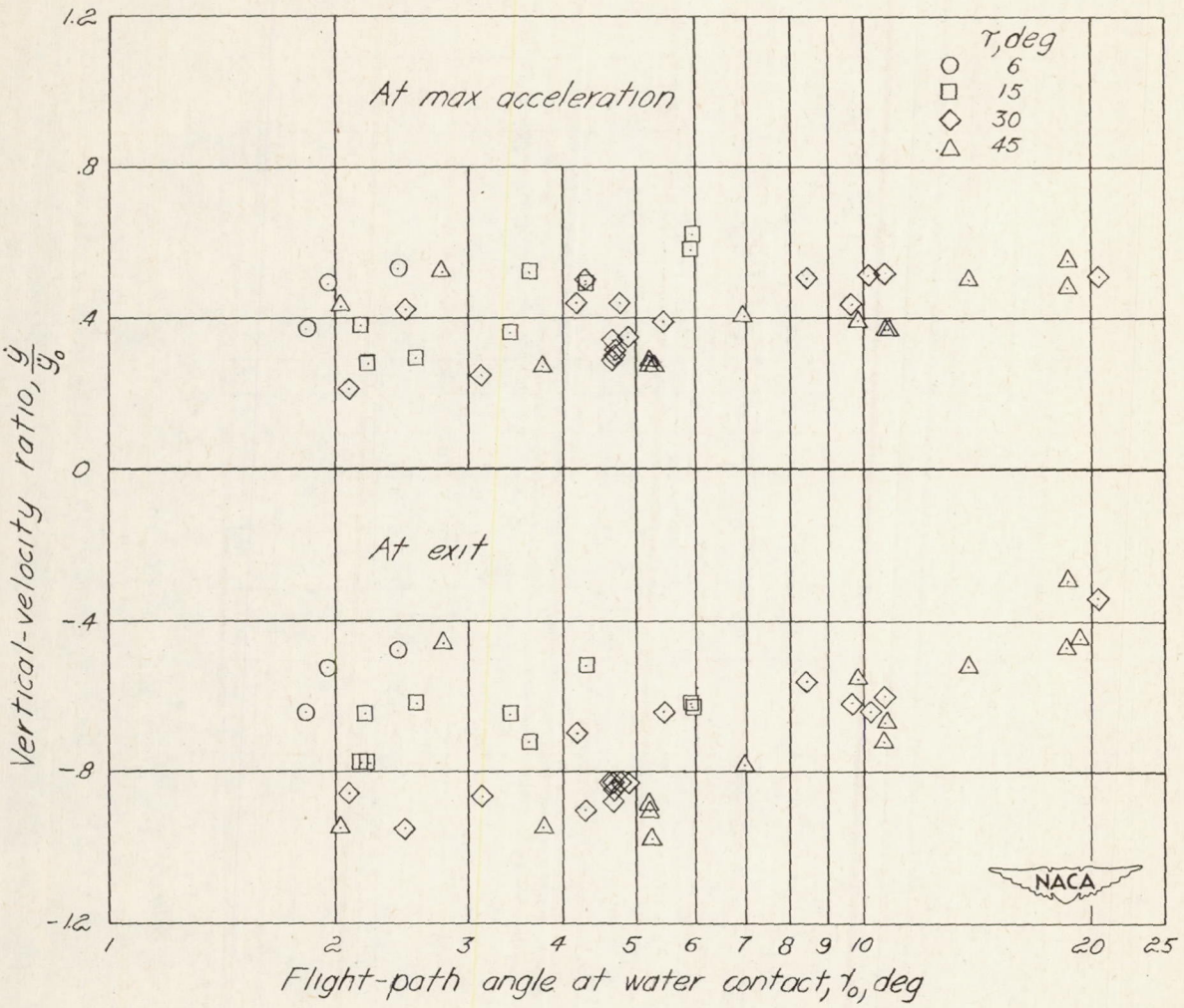

Figure 7.- Variation of vertical velocity with flight-path angle at water contact. $\beta = 30^\circ$; $C_\Delta = 18.8$.

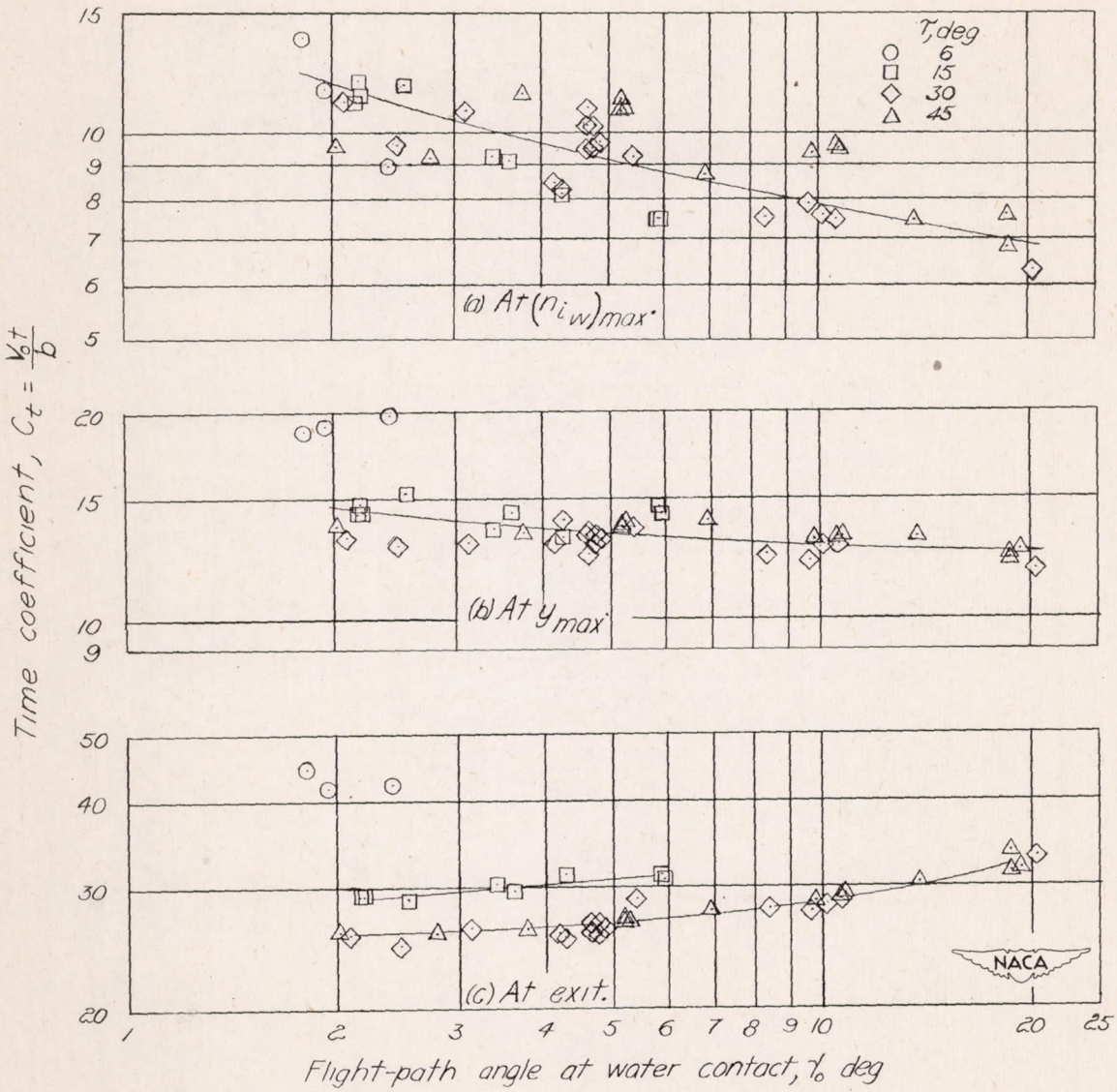

Figure 8.- Variation of time coefficient with flight-path angle at water contact. $\beta = 30^\circ$; $C_\Delta = 18.8$.

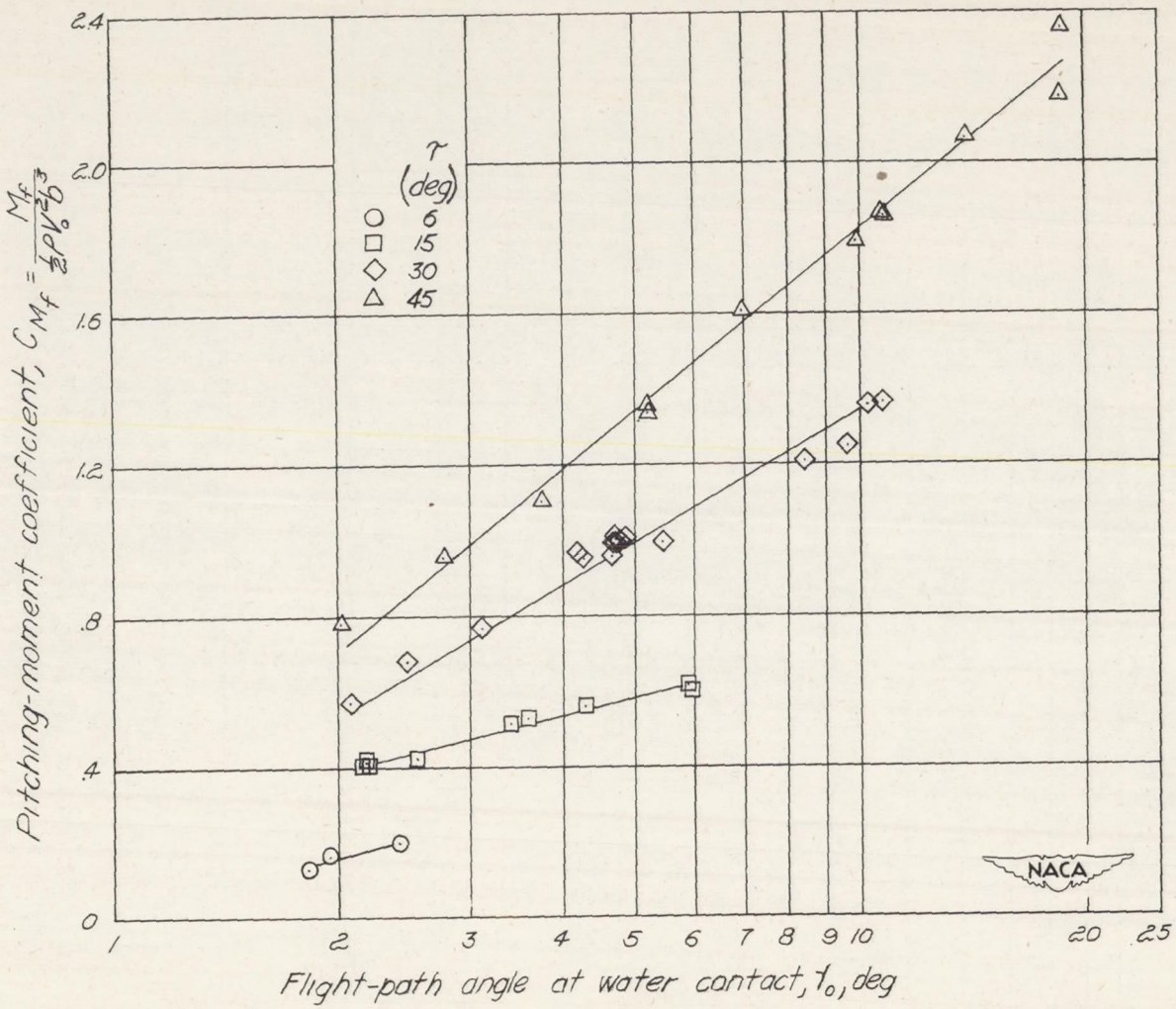

Figure 9.- Variation of pitching-moment coefficient referred to front fittings at time of $(n_{i_w})_{max}$ with flight-path angle at water contact. $\beta = 30^\circ$; $C_\Delta = 18.8$.

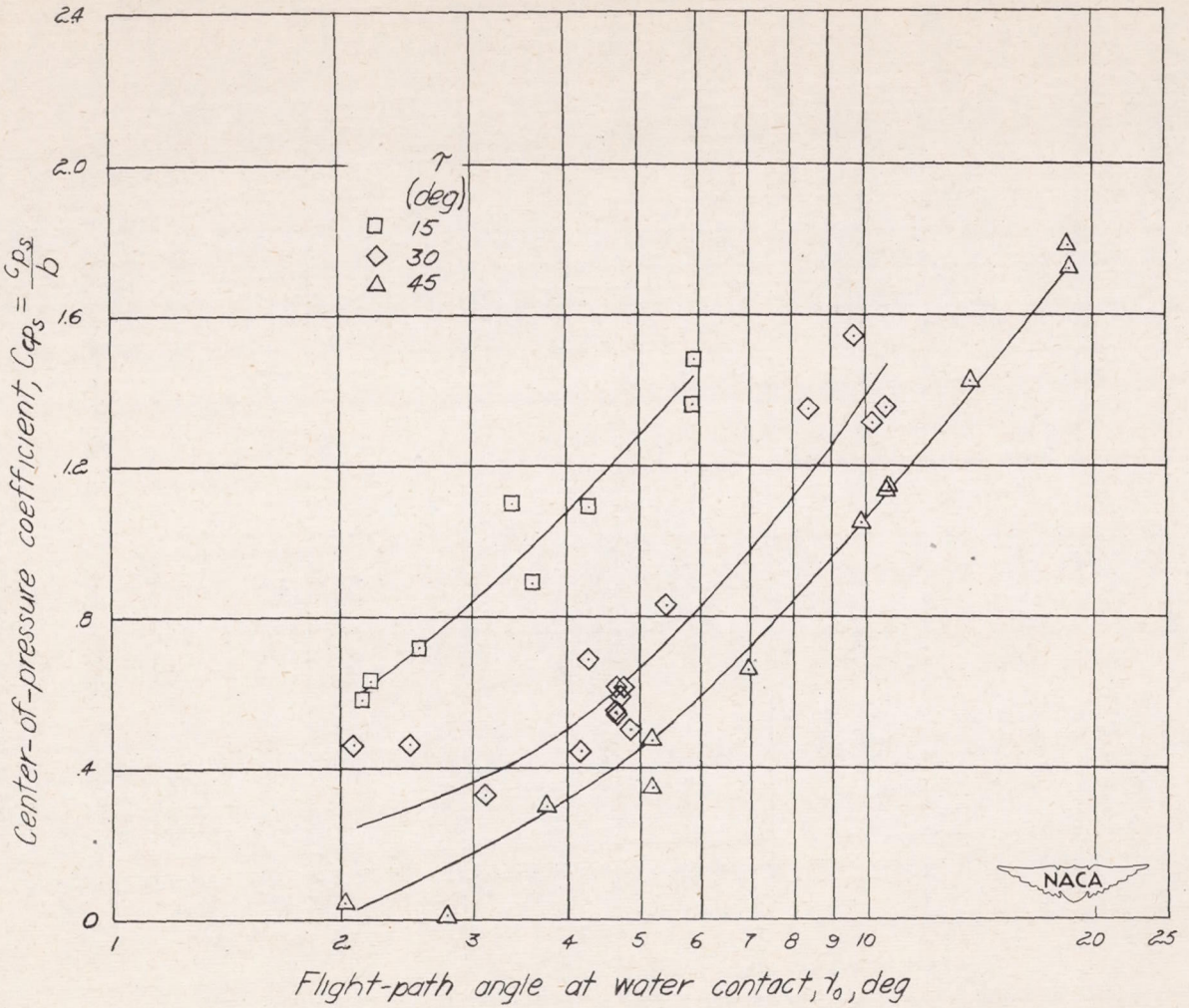

Figure 10.- Variation of center-of-pressure coefficient referred to step with flight-path angle at water contact. $\beta = 30^\circ$; $C_\Delta = 18.8$.

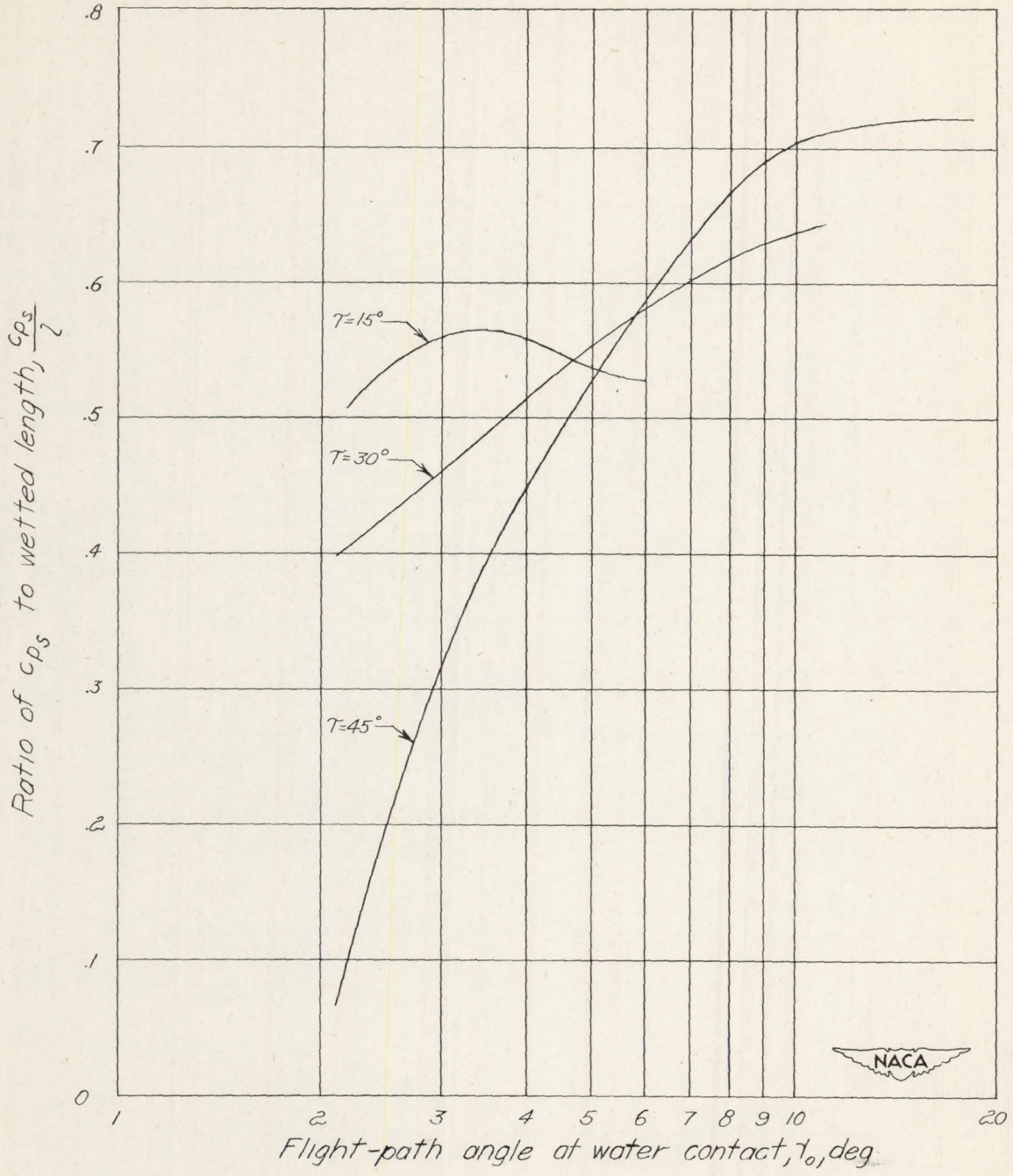

Figure 11.- Variation of ratio of c_{p_s} to wetted length with flight-path angle at water contact. $\beta = 30^\circ$; $C_\Delta = 18.8$.

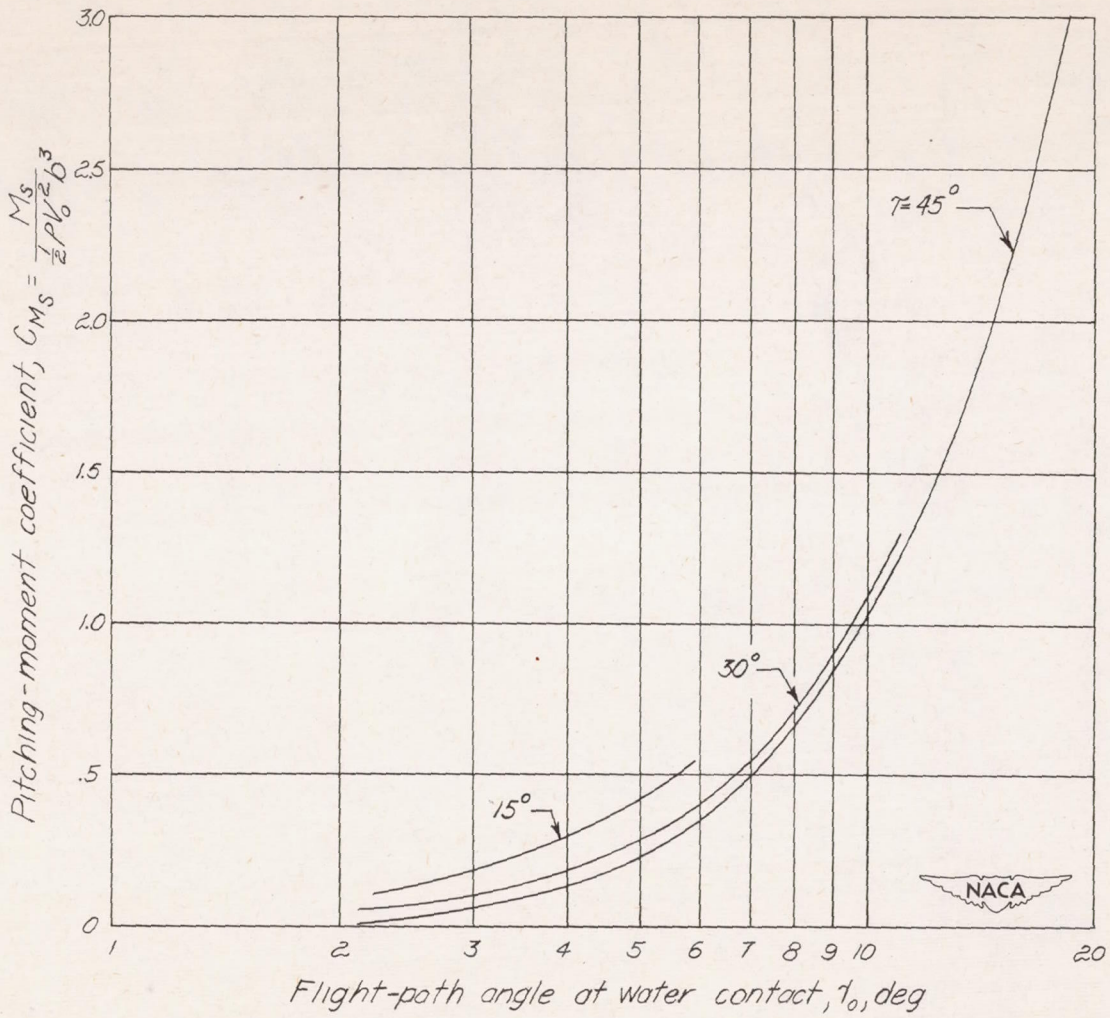

Figure 12.- Variation of pitching-moment coefficient referred to step at time of $(n_{i_w})_{max}$ with flight-path angle at water contact. $\beta = 30°$; $C_\Delta = 18.8$.